Norwegian University of Life Sciences
Faculty of Environmental Sciences and Natural Resource Management

2022

ISSN 2535-2806

MINA fagrapport 74

Estimates of wolverine density, abundance, and population dynamics in Scandinavia, 2013–2021

Cyril Milleret
Pierre Dupont
Henrik Brøseth
Øystein Flagstad
Jonas Kindberg
Richard Bischof

Milleret, C., Dupont, P., Brøseth, H., Flagstad, Ø, Kindberg, J., and Bischof, R., 2022. **Estimates of wolverine density, abundance, and population dynamics in Scandinavia, 2013–2021** - MINA fagrapport 74. 30 pp.

Ås, March 2022

ISSN: 2535-2806

AVAILABILITY

Open

PUBLICATION TYPE

Digital document (pdf)

QUALITY CONTROLLED BY

The Research committee (FU), MINA, NMBU

PRINCIPAL

Naturvårdsverket, Ref: NV-07883-21, Contact person: Robert Ekblom
Miljødirektoratet, Ref: 1/05424-1, Contact person: Terje Bø

COVER PICTURE

Wolverine, K. Bartik/Shutterstock.

NØKKELORD

Gulo gulo, jerv, tetthet, populasjonsdynamikk, deteksjonssannsynlighet, ikke-invaderende innsamling av genetisk materiale, åpen populasjon romlig fangst-gjenfangst, rovdyrforvaltning

KEY WORDS

Gulo gulo, wolverine, population density, population dynamics, detection probability, non-invasive genetic sampling, open-population spatial capture-recapture, carnivore management

Cyril Milleret, Faculty of Environmental Sciences and Natural Resource Management, Norwegian University of Life Sciences, PO Box 5003, NO-1432 Ås, Norway.

Pierre Dupont, Faculty of Environmental Sciences and Natural Resource Management, Norwegian University of Life Sciences, PO Box 5003, NO-1432 Ås, Norway.

Henrik Brøseth, Norwegian Institute for Nature Research, PO Box 5685, NO-7485 Trondheim, Norway.

Øystein Flagstad, Norwegian Institute for Nature Research, PO Box 5685, NO-7485 Trondheim, Norway.

Jonas Kindberg, Norwegian Institute for Nature Research, PO Box 5685, NO-7485 Trondheim, Norway.

Richard Bischof (richard.bischof@nmbu.no), Faculty of Environmental Sciences and Natural Resource Management, Norwegian University of Life Sciences, PO Box 5003, NO-1432 Ås, Norway.

Summary

Background The Scandinavian wolverine (*Gulo gulo*) population is being monitored annually using non-invasive genetic sampling (NGS) and recovery of dead individuals. DNA extracted from faeces, urine, hair, and tissue is used to identify the species, sex, and individual from which each sample originated. These data have been compiled in the Scandinavian large carnivore database Rovbase 3.0 (www.rovbase.se, www.rovbase.no).

Approach Using the Bayesian spatial capture-recapture (SCR) models developed by RovQuant (Bischof et al., 2019b, 2020b), we estimated annual density and vital rates of the Scandinavian wolverine population for nine seasons from 2013 to 2021. We used single-season SCR models to estimate abundance, except for Norrbotten (Sweden) where we used open-population SCR (OPSCR) models because sampling was not conducted comprehensively before 2017 and after 2019. The use of single-season SCR models was motivated by the fact that they make less assumptions compared to OPSCR models, and that their abundance estimates are relatively robust to model misspecifications. However, OPSCR models remain useful, as they allow estimation of vital rates and yield abundance estimates when there are gaps in monitoring.

Results Using single-season SCR and OPSCR models, we generated annual density maps and both total and jurisdiction-specific population sizes for wolverine from 2013 to 2021. Based on the spatial capture-recapture modelling approach, the Scandinavian wolverine population was likely (95% credible interval) between 1013 and 1126 individuals in 2021, with 639 to 724 individuals attributed to Sweden and 358 to 418 to Norway. In addition to annual density and jurisdiction-specific abundance estimates, we report annual estimates of survival, recruitment, and detection probabilities.

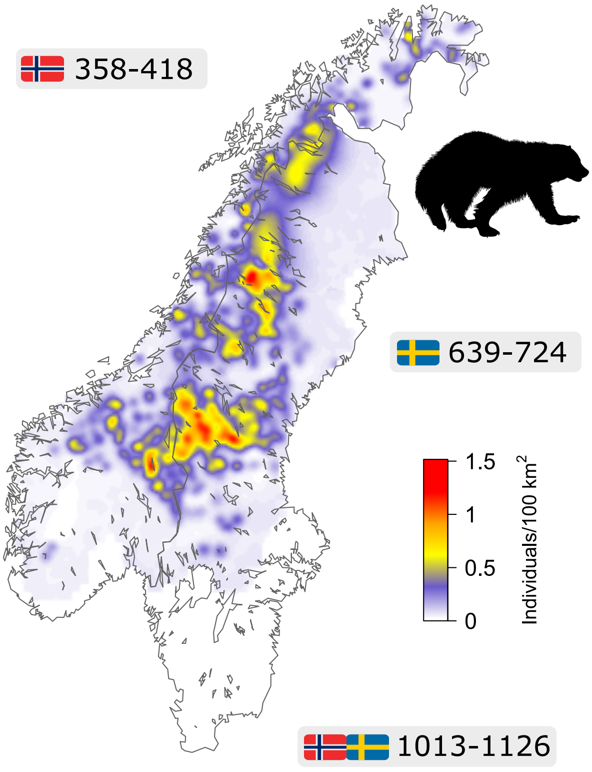

Density map and ranges of abundance estimated for wolverine in 2021

Sammendrag

Bakgrunn Den skandinaviske bestanden av jerv (Gulo gulo) blir overvåket årlig ved bruk av ikke-invasiv genetisk prøveinnsamling (NGS) og gjenfunn av døde individer. DNA ekstrahert fra skit, urin, hår og vev brukes til å identifisere art, kjønn og individ for hver enkelt prøve. Denne informasjonen samles og ivaretas i den skandinaviske databasen for store rovdyr; Rovbase 3.0 (www.rovbase.se ; www.rovbase.no).

Tilnærming Ved bruk av en Bayesiansk romlig fangst-gjenfangst modell (SCR), utviklet av RovQuant (Bischof et al., 2019b, 2020), estimerte vi årlige tettheter og demografiske rater hos den skandinaviske bestanden av jerv i ni sesonger fra 2013 til 2021. Vi brukte årlige SCR modeller for å estimere antall individer, bortsett fra i Norrbotten (Sverige) hvor vi brukte åpne SCR (OPSCR) modeller fordi det ikke var en omfattende prøveinnsamling før 2017 og etter 2019. Bruken av årlige SCR modeller var motivert ut fra det faktum at de inneholder færre antagelser sammenlignet med OPSCR modeller, samt at populasjonsestimatene er relativt robuste for feilspesifikasjoner i modellen. Men OPSCR modeller forblir nyttige da de gjør at man kan estimere demografiske rater mellom år og estimere populasjonsstørrelse når det er huller i dekningen på innsamlingen av prøver i overvåkingen.

Resultater Ved bruk av årlige SCR og OPSCR modeller er det laget skandinaviske kart med årlig tetthet av jerv fra 2013 til 2021, hvor bestandsstørrelsen både totalt og innenfor ulike administrative geografiske områder kan avledes. Basert på den romlige fangst-gjenfangst modelleringen estimeres den skandinaviske populasjonen av jerv til mellom 1013 og 1126 individer i 2021 (95% credible interval), med 639 til 724 individer i Sverige og 358 til 418 i Norge. I tillegg til årlig tetthet og bestandsstørrelse i ulike administrative geografiske områder er det beregnet årlige estimater på overlevelse, rekrutering og oppdagbarhet.

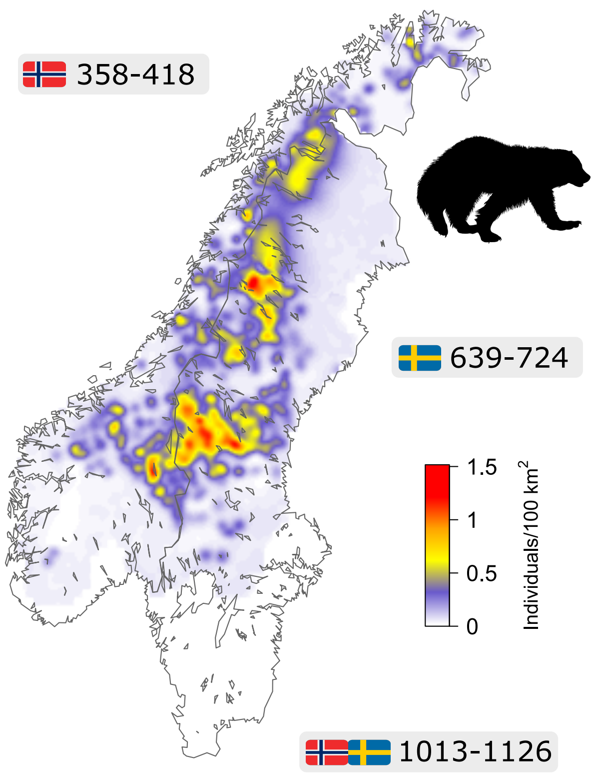

Kart som viser tetthet av jerv i 2021 sammen
med intervaller for estimert antall jerv

Contents

1 Introduction

Non-invasive genetic sampling (NGS) and dead recoveries, are a centerpiece of national and regional large carnivore monitoring in Norway and Sweden. Over almost two decades, both countries have accumulated an extensive individual-based data set for wolverines (*Gulo gulo*), and plan to continue such trans-national monitoring in the future.

Since 2017, project RovQuant has been developing statistical methods that allow a comprehensive assessment of the status and dynamics of large carnivore populations using NGS data and other sources of information collected and stored in Rovbase (www.rovbase.se, www.rovbase.no) by the national monitoring programs in Sweden and Norway. At the core of the analytical framework developed by RovQuant (Bischof et al., 2019b, 2020b) are Bayesian spatial capture-recapture (SCR) and open-population spatial capture-recapture (OPSCR) models (Ergon and Gardner, 2014; Bischof et al., 2016; Chandler et al., 2018).

Rovquant reported its first results for wolves in March 2019 (Bischof et al., 2019a), jointly for all three carnivore species in December 2019 (Bischof et al., 2019b, 2020b), and for wolves (Milleret et al., 2021b) and wolverines in 2020 (Flagstad et al., 2021). Here we repeat the analysis for wolverines, adding the latest NGS and dead-recovery data from 2021, for a total of nine monitoring seasons (2012/13–2020/21). We do so with the goal to provide the following information:

- Estimated number of wolverines (with credible intervals) for Sweden, Norway, and both countries combined, as well as estimates by county in Sweden and large carnivore management regions in Norway.
- Estimated proportion of individuals detected through NGS.
- Wolverine density map throughout the species' primary range in Scandinavia.
- Annual estimates of mortality, recruitment, and population growth rate.

Since 2017, Rovquant developed and used several single-season SCR and OPSCR models. While OPSCR models are relatively recent and their robustness to violations of assumptions is still relatively unknown, single-season SCR models have been more thoroughly tested and several studies suggest that estimates of abundance from single-season SCR models are relatively robust to model misspecifications (Bischof et al., 2020a; Moqanaki et al., 2021; Dupont et al., 2019; Dey et al., 2022; Theng et al., 2022). Single-season SCR models have the advantage of making fewer assumptions about the underlying processes since vital rates and inter-annual movement are not estimated. Single-season SCR models are therefore the more conservative approach for obtaining estimates of abundance. However, a key limitation of single-season SCR models is that they ignore information available from preceding and subsequent years, and are thus unable to fill temporal and spatial gaps in sampling. OPSCR models, on the other hand, can fill those gaps (Milleret et al., 2020). We therefore used a combination of both single-season SCR and OPSCR models to obtain comprehensive abundance estimates and fill spatio-temporal gaps in monitoring.

Box 1: Definitions and acronyms

AC: Activity center. Equivalent to the center of an individual's home range during the monitoring period. "AC location" refers to the spatial coordinates of an individual AC in a given year, and "AC movement" to the movement of an individual AC between consecutive years.

CrI: 95% credible interval associated with a posterior sample distribution.

Detectors: Potential detection locations in the spatial capture-recapture framework. These can refer to fixed locations (e.g. camera-trap locations) or to areas searched (e.g. habitat grid cells where searches for genetic samples were conducted) as used in this project.

Statsforvalteren: Norwegian state's representative in the county, responsible for following up decisions, goals, and guidelines from the legislature and the government.

Habitat buffer: Buffer surrounding the searched area that is considered suitable habitat but was not searched.

Legal culling: Lethal removal of individuals by legal means including licensed recreational hunting, management removals, defense of life and property.

Länsstyrelserna: Swedish County Administrative Boards, in charge of the monitoring of large carnivores at the county level.

MCMC: Markov Chain Monte Carlo.

NGS: Non-invasive genetic sampling.

OPSCR: Open-population spatial capture-recapture.

p0: Baseline detection probability; probability of detecting an individual at a given detector, if the individual's AC is located exactly at the detector location.

$\boldsymbol{\sigma}$: Scale parameter of the detection function; related to the size of the circular home-range.

SCR: Spatial capture-recapture.

SNO: Statens naturoppsyn (Norwegian Nature Inspectorate) is the operative field branch of the Norwegian Environment Directorate (Miljødirektoratet).

2 Methods

2.1 Data

We relied on data from multiple sources, the primary one being the Scandinavian large carnivore database Rovbase 3.0 (rovbase.se and rovbase.no; last extraction: 2021-10-29). This database is used jointly by Norway and Sweden to record detailed information associated with large carnivore monitoring, including, but not limited to, non-invasive genetic sampling (NGS) data, dead recoveries, and GPS search tracks. In the following sections, we describe the various types of data used in the analysis. We used data collected during winters 2012/13 to 2020/2021.

Non-invasive genetic sampling In Norway, the collection of wolverine scat and hair is managed at the level of counties by SNO. Sample collection is conducted by SNO field officers, wardens at Statskog Fjelltjenesten (statskog.no), wardens at Fjellstyrene (fjellstyrene.no), local predator contacts, hunters and other members of the public. Rovdata (rovdata.no), an unit within the Norwegian Institute for Nature Research, has responsibility for the Norwegian large carnivore monitoring program. In Sweden, the collection of scat and hair is managed by Länsstyrelserna at the regional level and carried out by field officers from Länsstyrelserna. NGS collection was conducted primarily between Dec 1 and June 30 each year. DNA was isolated using a manual method originally developed to isolate DNA from soil samples (PowerMax®Soil DNA Isolation Kit, MO BIO Laboratories, Carlsbad, California, USA). After DNA isolation and identification of genus-specific DNA in the sample, DNA profiles were generated from 12 microsatellite markers. Samples with identical DNA profiles were classified as the same individual. In addition to the 12 markers, all individuals (one sample per individual) were analyzed for an additional 7 markers. For further details on the DNA analysis procedure see Flagstad et al. (2004), Flagstad et al. (2021), and Kleven et al. (2022).

Dead recoveries All large carnivores killed legally in Scandinavia (e.g., legal hunting, management kills, defense of life and property) have to be reported to the management authorities (Statsforvalteren or SNO in Norway and Länsstyrelserna or the police in Sweden). Although some mortalities due to other reasons (e.g., natural deaths, vehicle and train collisions, illegal hunting) are also reported, an unknown proportion remains undetected. Tissue is collected from all reported dead carnivores for DNA extraction and analysis. DNA from dead carnivores, if genotyped, can be linked with NGS data via individual IDs and provide definite information about the fate of individuals. Dead recoveries associated with geographic coordinates also provide additional information for the estimation of individual locations, especially valuable for individuals with few or no NGS detections (Dupont et al., 2021).

GPS search tracks Government employees involved in structured searches for wolverine DNA (e.g., via snowmobiles, skis, snowshoes, etc.) documented their effort with GPS track logs which were registered in Rovbase 3.0. GPS search tracks were included in the analysis to account for spatial and temporal variation in search effort.

2.2 Data analysis

Previously, we used OPSCR models to generate annual abundance estimates of wolves, bears and wolverines (Bischof et al., 2019b, 2020b; Milleret et al., 2021b; Flagstad et al., 2021). OPSCR models have the advantage of integrating NGS and dead-recovery data from multiple consecutive years and can thus estimate vital rates and individual movements between monitoring seasons in addition to annual density. OPSCR models are relatively new and the consequences that misspecified vital rate and movement sub-models have for abundance estimates are poorly known.

On the other hand, the sensitivity of single-season SCR models to violations of assumptions has been explored extensively (Bischof et al., 2020a; Moqanaki et al., 2021; Dupont et al., 2019; Dey et al., 2022; Theng et al., 2022), and abundance estimates from SCR models are generally considered robust to model misspecification. In this analysis, we therefore relied primarily on RovQuant's single-season Bayesian spatial capture-recapture (SCR; Bischof et al. 2019b) and NGS data. In addition, we complemented the analysis with OPSCR models, as these a) can yield estimate of vital rates and b) are able to bridge spatio-temporal gaps in sampling (Bischof et al., 2019b; Milleret et al., 2020). OPSCR models incorporate population dynamics, exploit data across multiple years with sampling (e.g., before and after gaps), and use the extra information provided by spatial dead recoveries (Bischof et al., 2019b; Milleret et al., 2020; Dupont et al., 2021).

Practically, this means that we fitted 9 single-season SCR models (one per season) and one OPSCR model to the entire 9-year data time-series. The OPSCR allowed us to estimate vital rates, but also density in regions with no comprehensive sampling. The single-season SCR models were used to estimate abundance in all regions with comprehensive sampling. The spatial domain, location of the detectors, definition of the covariates, and the model for the detection process were similar between the single-season SCR and OPSCR models.

Single-season spatial capture-recapture model The SCR model is composed of two sub-models, one for the spatial distribution of individuals in the population, and one for detections of individuals during NGS searches. The first sub-model accounts for spatial variation in density by using counts of known wolverine dens as a spatially-explicit covariate on the number of individual activity centers (Bischof et al., 2019a,b, 2020b; Milleret et al., 2021a). The second sub-model accounts for spatial variation in detection probability by using:

- Spatial-variation in individual detection probability based on the distance between activity center positions (estimated by the density sub-model) and a given detector. A half-normal function was used to express the declining probability of detection with increasing distance between the AC and the detector.
- Spatial-variation in effort using the length of GPS search tracks. For years and areas without comprehensive sampling effort (Norrbotten county in Sweden in all years except 2017, 2018, and 2019), we removed all samples collected within the county and fixed detection probability to 0.
- Spatial variation in accessibility with the average distance from the nearest road.
- Spatio-temporal variation in snow cover.
- Spatio-temporal variation linked with differences in monitoring regimes between jurisdictions (counties).
- Individual variation linked with a previous detection that could be expected to positively influence the probability of being detected at subsequent occasions

The different model components and data sources for covariates are described in detail in Bischof et al. (2019a), Bischof et al. (2019b), and Bischof et al. (2020b).

Open-population spatial capture-recapture model The OPSCR model was similar to the single-season SCR model described above, with the exception that the model on density also included a movement model between years and a state transition model. The state-transition model allowed the integration of spatial dead recoveries (Dupont et al., 2021), to estimate annual cause-specific mortalities, and annual recruitment probabilities (see details in Bischof et al. (2019a), Bischof et al. (2019b), and Bischof et al. (2020b)). Individual or spatial variation in movement and vital rates are currently not accounted for in the OPSCR model. This is a development RovQuant is currently working on (Milleret et al., 2022).

Model fitting We fitted the Bayesian SCR and OPSCR models using Markov chain Monte Carlo (MCMC) simulation with NIMBLE (Turek et al., 2021; de Valpine et al., 2017; NIMBLE Development Team, 2019) and nimbleSCR (Bischof et al., 2021) in R version 3.3.3 (R Core Team, 2018). We ran 4 chains for both OPSCR and SCR models. For SCR models, we used 20 000 iterations, including a 10 000-iterations burn-in period. OPSCR models, being more complex, require longer runs. For these, we used 37 500 iterations, including a 12 500-iterations burn-in period. Due to the computing challenge associated with post-processing large amounts of data, we thinned chains by a factor of 10 from which abundance estimates were derived. We considered models as converged when the Gelman-Rubin diagnostics (Rhat, Gelman and Rubin, 1992) was ≤ 1.1 for all parameters and by visually inspecting the trace plots.

Abundance estimates To ensure that abundance estimates for spatial sub-units (jurisdictions) add up to the overall abundance estimate, we used the mean and associated 95% credible interval limits to summarize posterior distributions of abundance. Combined (female/male) parameter estimates were obtained by merging posterior samples from the sex-specific models.

To obtain an estimate of abundance for any given area, we summed the number of predicted AC locations (live individuals) that fell within that area for each iteration of the MCMC chains, thus generating a posterior distribution of abundance for that area. In this fashion, abundance estimates and the associated uncertainty can be extracted for any spatial unit, including countries or counties.

Norrbotten county in Sweden was comprehensively searched only during years 2017, 2018, and 2019. County-wide single-seaons SCR estimates of abundance could only be obtained for those years. For the remaining years (2013, 2014, 2015, 2016, 2020, and 2021), abundance for Norrbotten was estimated using OPSCR models. In those years, Swedish and Scandinavia-wide estimates are therefore derived from a combination of SCR- and OPSCR-produced estimates.

Technically, this was accomplished by 1) calculating the model-predicted number of activity centers in each habitat cell (for both the SCR and the OPSCR models), 2) subsampling the posterior samples produced by the OPSCR model to the same number of posterior samples as the SCR model, 3) combining the posterior cell-based AC counts from the OPSCR model for cells in Norrbotten with the posterior cell-based AC counts from the SCR models in all other regions, and 4) calculating region-specific means and 95% credible intervals from the cell-based posteriors associated with a given region.

Density maps We used both the distribution of model-estimated AC positions and the scale parameter (σ) of the detection function to construct density maps based on individual utilization distributions. These maps are not only based on the position of the center of an individual's home range, but also take into account the area over which that individual's activity is spread, i.e., its space use (Bischof et al., 2020b). To do so, we constructed raster maps (5 km resolution) of individual utilization distributions, scaled values in each raster to sum to one, and then summed rasters across individuals to create a single population-level raster map for each iteration. An overall density map was derived by calculating the mean across iterations in each cell (Bischof et al., 2020b). Density maps for the Norrbotten region were obtained using OPSCR models in 2013, 2014, 2015, 2016, 2020, and 2021, while estimates for the remaining years and the rest of the Swedish counties and Norwegian regions were obtained using SCR models.

Derived parameters The average proportion of individuals detected and the associated uncertainty were obtained by dividing the number of individuals detected through NGS sampling (Table A.2) by the abundance estimates and their associated credible intervals, respectively.
We derived the proportion of females in the population and the associated uncertainty by dividing the posterior distribution representing the number of females by the combined abundance estimate for males and females (Table A.2). Growth rate (λ; Table A.5) was calculated as $\lambda_t = N_{t+1}/N_t$.

Focus on uncertainty Although we reported median (or mean for abundance; see below) estimates for all parameters in the tables, we intentionally focused the main results of our report on the 95% credible interval limits of the posterior distributions. We did so with the aim of drawing the reader's attention to the uncertainty around population size estimates, rather than a single point estimate.

3 Results

3.1 Non-invasive genetic samples and dead recoveries

A total of 17 512 (7 871 female; 9 641 male) genotyped wolverine genetic samples were included in the analysis, of which 41% originated from Sweden. These samples were associated with 2 520 (1337 female; 1183 male) individuals. We also used 1035 dead recoveries of wolverines in the OPSCR model, of which 972 (477 female; 495 male) were due to legal culling and 63 (27 female; 36 male) due to other causes of mortality. The majority of dead recoveries (83%) originated from Norway. Annual total and country-specific tallies of NGS samples and associated individuals, as well as dead recoveries included in the analysis are provided in the Appendices (NGS samples: Table A.1, NGS individuals: Table A.2, dead recoveries: Table A.3)

3.2 Density and abundance

Wolverine abundance for the entire study area (619 550 km^2, excluding the buffer area) was estimated (95% credible interval) between 1 013 and 1 126 individuals in 2021 (Table 1). Estimates refer to the status of the population at the start of the annual sampling period (Dec. 1). The proportion of females in the Scandinavian wolverine population was likely between 62% and 66% in 2021. Based on the model-predicted location of ACs, we estimated that in 2021, between 639 to 724 individuals were attributed to Sweden and 358 to 418 to Norway (Table 1). See Table 1 for total and sex-specific estimates for each country and management area. See Table A.4 for annual estimates for all of Scandinavia and by region between 2013 and 2021. Note that estimates for different years shown here differ slightly from those provided in Bischof et al. (2020b) and Flagstad et al. (2021). This is due to the use of separate single-season SCR models in the present analysis, instead of OPSCR models that analyze data jointly from multiple years. The analysis yielded annual density maps, which illustrate changes in the distribution of wolverines over time (Figure A.2, Figure A.3). Overall wolverine density in 2021 was likely between 0.16 and 0.18 km^2 per 100 km^2 throughout the study area (Figure 1).

Table 1: Wolverine population size estimates by sex and jurisdiction (Norway: carnivore management regions, Sweden: counties) in 2021. Readers should focus on the 95% credible interval provided in parentheses, as these - unlike mean values - convey uncertainty inherent in abundance estimates. Numbers are based on estimated activity center locations of wolverines. Combined female-male estimates were obtained by joining sex-specific posterior distributions. Rounding may result in small deviations between total estimates and the sum of the estimates for constituent regions. Values without a star are based on single-season spatial-capture recapture (SCR) models. Estimates for Norrbotten county in years without comprehensive non-invasive genetic sampling were derived using an open-population spatial capture-recapture (OPSCR) model (shown in grey and marked with $*$). Estimates marked with $**$ are based on a combination of OPSCR estimates for Norrbotten county and single-season SCR estimates for all other jurisdictions. See the Methods section for further detail.

	Females	Males	Total
TOTAL**	684 (633-738)	383.5 (362-407)	1067.4 (1013-1126)
NORWAY	246 (220-276)	140.4 (129-153)	386.4 (358-418)
Region 1	11.3 (5-19)	3.5 (1-7)	14.7 (7-23)
Region 2	8.6 (3-15)	2.5 (0-6)	11.2 (5-18)
Region 3	21.6 (17-28)	11.9 (9-15)	33.5 (28-40)
Region 4	3.2 (0-7)	0.8 (0-3)	4 (1-9)
Region 5	44.8 (38-53)	36.4 (32-41)	81.2 (73-91)
Region 6	54.3 (45-65)	29.5 (24-36)	83.9 (73-96)
Region 7	39 (32-47)	24.5 (21-28)	63.5 (56-72)
Region 8	63 (51-77)	31.3 (27-37)	94.4 (82-109)
SWEDEN**	438 (402-477)	243 (224-263)	681 (639-724)
Örebro	3.9 (1-8)	1.1 (0-3)	5 (1-10)
Östergötland	0 (0-0)	0 (0-0)	0 (0-0)
Dalarna	32.3 (25-40)	19.7 (16-24)	51.9 (44-61)
Gävleborg	11.8 (8-17)	13.5 (10-17)	25.3 (20-31)
Jämtland	135.6 (121-152)	81.1 (74-89)	216.7 (200-234)
Norrbotten*	124.3 (102-147)*	59.3 (45-75)*	183.6 (157-212)*
Södermanland	0 (0-1)	0 (0-0)	0.1 (0-1)
Värmland	7.5 (3-13)	5.8 (3-9)	13.4 (8-20)
Västerbotten	95.1 (79-114)	45.8 (39-54)	140.9 (123-161)
Västernorrland	25.2 (20-32)	15.9 (12-20)	41.1 (34-49)
Västmanland	1.2 (0-4)	0.4 (0-2)	1.6 (0-5)
VästraGötaland	1.1 (0-3)	0.4 (0-2)	1.5 (0-4)

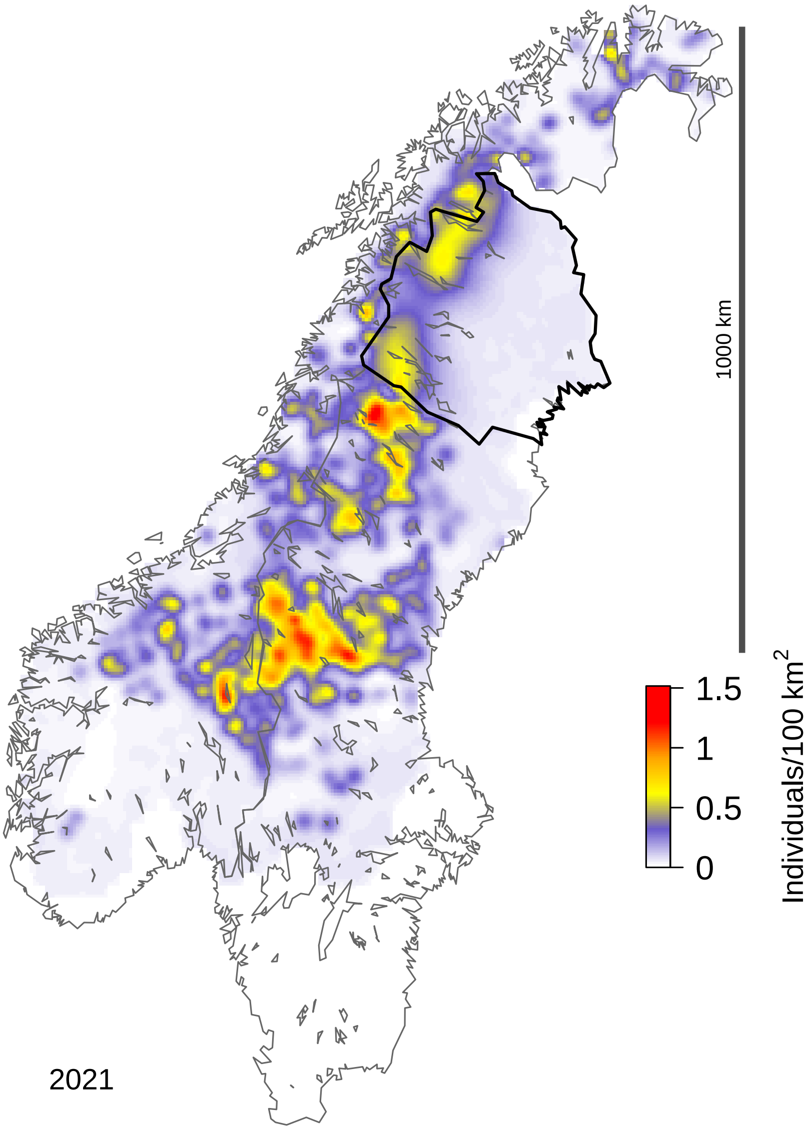

Figure 1: Wolverine density based on individual utilization distributions throughout the study area in Scandinavia in 2021. With the exception of Norrbotten county (black outline), density was estimated with a single-season spatial-capture recapture model fitted to DNA data collected in 2021. Because Norrbotten county was not sampled comprehensively in 2021, density in this county had to be estimated using the open-population spatial capture-recapture (OPSCR) model. The OPSCR model can be used to fill gaps in density and abundance estimates by incorporating population dynamics and using information in years with sampling. See Methods section for further detail.

3.3 Vital rates

The OPSCR model produced annual estimates of legal hunting mortality, mortality associated with all other causes, and per capita recruitment rates (Figure 2; Table A.6). We have fitted OPSCR models to wolverine data during the past three years, each year updating the input data with the latest information from the monitoring program: 2019 (Bischof et al., 2020b), 2020 (Flagstad et al., 2021) and 2021 (this report). For the most part, annual vital rate estimates for past years remained nearly unchanged when analyses were updated with new data. However, vital rate estimates for the final time step (transition) of a given time series, showed a pronounced shift each time the analysis was extended with a new annual data set (Figure 2, Figure 3). For example, vital rate estimates obtained for the transition from 2018 to 2019 were different for the OPSCR model fitted to the data collected between 2012-2019 and the OPSCR model fitted to data collected between 2012-2020 (one extra year of monitoring data; Figure 2, Figure 3). This pattern was consistent across the three OPSCR models fitted over the past three years (Figure 2, Figure 3). Differences were most pronounced for other causes of mortality and recruitment, but not legal culling (Figure 2, Figure 3). We are currently exploring whether this is the result of a model misspecification (e.g., in the population dynamic or movement components) or an artifact of how the model uses information in the final year of the time series.

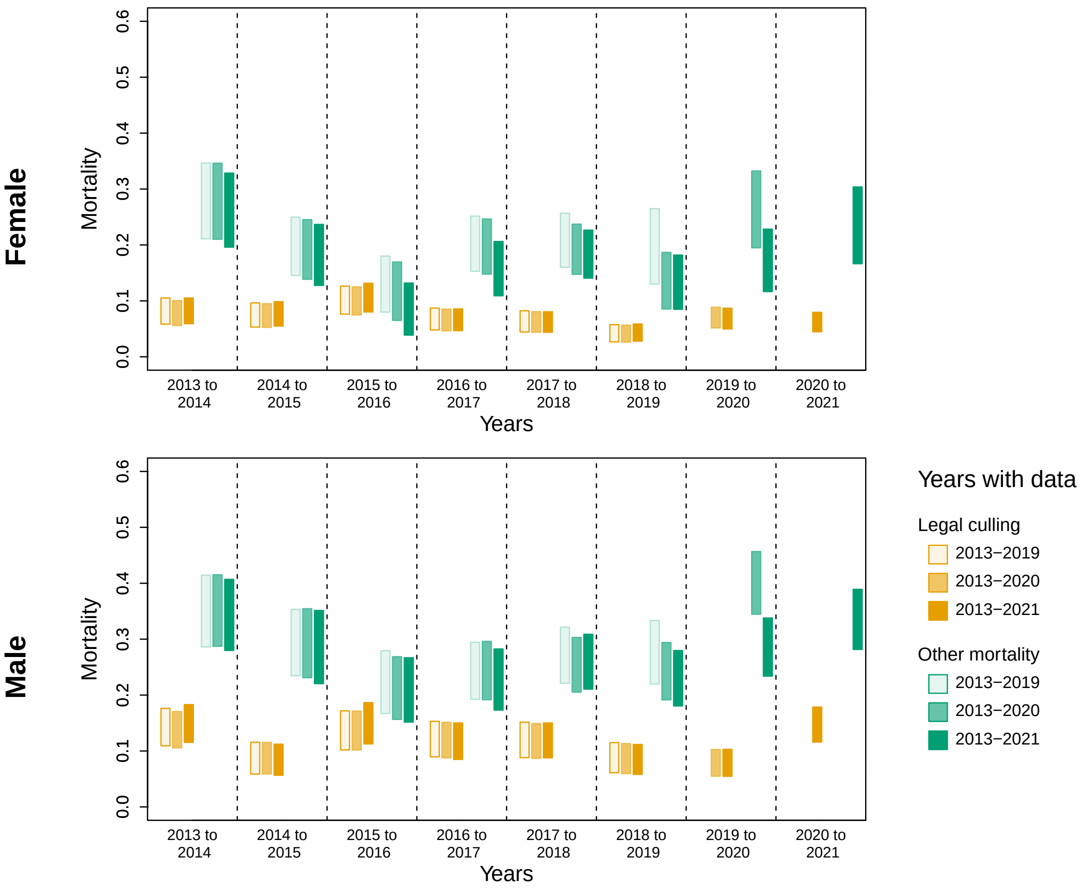

Figure 2: Mortality probabilities due to legal culling (orange) and all other causes (green) for female and male wolverines. Shown are overall estimates throughout the study area, based on three different OPSCR analyses with progressively longer time series of NGS and dead-recovery data: 2013–2019, 2013–2020, and 2013–2021. Darker shading indicates longer time series. Bars represent the 95% credible interval. Estimates refer to deaths occurring between the start of one sampling season and the start of the next.

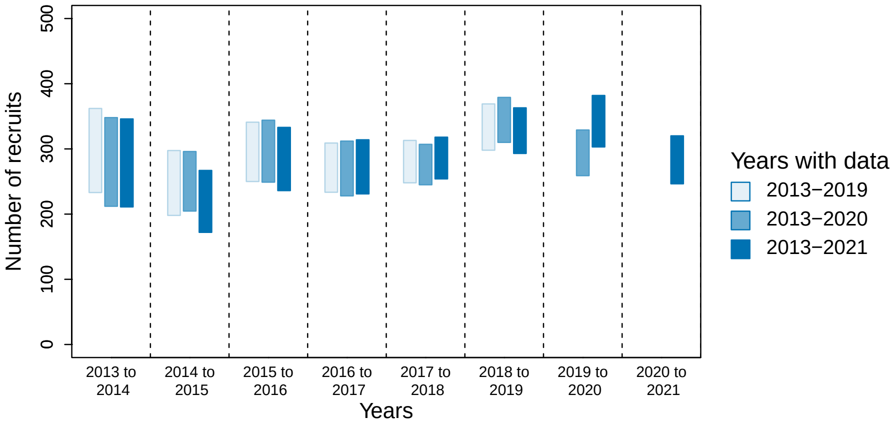

Figure 3: Estimated annual number of recruits. Shown are overall estimates throughout the study area, based on three different OPSCR analyses with progressively longer time series of NGS and dead-recovery data: 2013–2019, 2013–2020, and 2013–2021. Darker shading indicates longer time series. Bars represent the 95% credible interval. Estimates refer to number of individuals recruited between the start of one sampling season and the start of the next.

3.4 Detection probability

The overall proportion of individuals in the population detected was likely between 56% and 63% in 2021 (Table A.8). The baseline detection probability (p_0) varied between jurisdictions and was the highest in 2018 (Figure A.4), which was also reflected with the largest proportion of individuals detected in that year (79% - 86%; Table A.8). Detection probability increased with the length of recorded search trails (2021; males: $\beta = 0.50$, CrI: 0.43 - 0.58; females: $\beta = 0.54$, CrI: 0.45 - 0.62; Table A.7). The effect of the distance to roads on p_0 was not significant in 2021. However, detectability tended to decrease in areas further away from roads for both males and females in other years (Table A.7). The average proportion of snow cover had a positive effect on the baseline detection probability for both sexes (2021; males: $\beta = 0.15$, CrI: 0.02 - 0.28; females: $\beta = 0.26$, CrI: 0.11 - 0.42; Table A.7). Detection probability was also generally higher for individuals if they had already been detected during the previous sampling season especially for males (2021; males: $\beta = 0.47$, CrI: 0.30 - 0.64; females: $\beta = 0.01$, CrI: -0.20 - 0.22; Table A.7).

4 Concluding remarks

SCR models, like the ones used in this analysis, address two primary challenges associated with wildlife monitoring:

- **Imperfect and variable detection probability:** Not all individuals present in the study area are detected and the probability of detection varies across space. This has multiple reasons, including variation in sampling effort and the location of animals relative to searched areas. SCR models models can account for important sources of variation in detection probability and produce estimates of total population size that include individuals that were never detected.

- **Difficulty defining the spatial extent:** Carnivores move, and the same individual may be detected in multiple, sometimes distant, locations. As a consequence, individuals that reside primarily outside the surveyed area may be detected within it. This makes it exceedingly difficult for traditional analytical methods to identify the area from which animals are sampled during wildlife surveys. SCR solves this problem and can estimate density by linking abundance with a spatial extent.

OPSCR models, an extension of SCR models, deal with one additional important challenge in the analysis of long-term monitoring data:

- **Entanglement of survival and recruitment with emigration and immigration:** Non-spatial population dynamic models estimate apparent survival and recruitment, as these parameters include the probability of permanent emigration and immigration, respectively. By explicitly modeling movement of individuals between years, OPSCR models can return unbiased estimates of demographic parameters (Ergon and Gardner, 2014; Gardner et al., 2018).

OPSCR models, apart from estimating vital rates and individual movement, offer other advantages, such as the use of multiple consecutive years of data, the propagation of information across years, and the option to exploit dead recovery data (Bischof et al., 2020b; Milleret et al., 2020; Dupont et al., 2021). However, OPSCR models are relatively new and still suffer from a lack of efficient ways to integrate spatial and individual variation in demographic rates and movement of individuals. For this reason, during the analysis described here, we combined abundance estimates obtained from single-season SCR models and an OPSCR model. The OPSCR model was used to obtain vital rates estimates and fill the gaps in abundance estimates in areas and years that were not comprehensively sampled (Bischof et al., 2020b; Milleret et al., 2020). Basing abundance estimates and their associated uncertainty on two different models is not ideal, but we chose this approach as it relied primarily on more robust single-season SCR models while estimating abundance for poorly-sampled regions by propagating information across years with the OPSCR model.

In addition to the aforementioned combined use of SCR and OPSCR models, the analyses described in this report included the following adjustment compared with previous analyses of wolverine density in Scandinavia (Bischof et al., 2020b; Flagstad et al., 2021): The extent of the area (habitat) for which estimates were generated has been increased and is now identical for male and female wolverines.

RovQuant continues to test and extend the functionality of SCR and OPSCR models. We aim to incorporate the following developments in future SCR analyses of the Scandinavian wolverine monitoring data:

1. Review and adjust spatial covariates on density. This may involve the addition of land cover and topographic variables.

2. Distinguish between dispersing and non-dispersing individuals, for example by using a finite-mixture approach.

3. Consider alternative detection models that do not assume a half-normal and/or circular home ranges.

We have recently been able to account for spatial variation in survival in an OPSCR model (Milleret et al., 2022). This is an important development, even if it not yet computationally feasible for implementation at the scale of Scandinavia. Once OPSCR models have gone through additional validation and achieved acceptable biological realism, we may again deploy them as stand-alone tools for wolverine abundance estimation.

5 Acknowledgements

This work was made possible by the large carnivore monitoring programs and the extensive monitoring data collected by Swedish (Länstyrelsena) and Norwegian (SNO) wildlife management authorities, as well as the public in both countries. Our analyses relied on genetic analyses conducted by the laboratory personnel at the DNA laboratories at the Swedish University of Agricultural Sciences, the Norwegian Institute for Nature Research, and the Uppsala University. We also thank Swedish and Norwegian wildlife managers for feedback provided during project RovQuant and the Research Council of Norway for partial funding (NFR 286886; project WildMap). The computations/simulations were performed on resources provided by NMBU's computing cluster "Orion", administered by the Centre for Integrative Genetics and by UNINETT Sigma2 - the National Infrastructure for High Performance Computing and Data Storage in Norway. We are grateful to P. de Valpine and D. Turek for help with the formulation of the OPSCR model in Nimble. J. Vermaat provided helpful comments on drafts of this report.

6 Data availability

Data, R code to reproduce the analysis, as well as figures, tables, and raster maps (Figure A.3) are available on GitHub https://github.com/richbi/RovQuantPublic

References

Bischof, R., Brøseth, H., and Gimenez, O. (2016). Wildlife in a Politically Divided World: Insularism Inflates Estimates of Brown Bear Abundance. *Conservation Letters*, 9(2):122–130.

Bischof, R., Dupont, P., Milleret, C., Chipperfield, J., and Royle, J. A. (2020a). Consequences of ignoring group association in spatial capture–recapture analysis. *Wildlife Biology*, 2020(1).

Bischof, R., Milleret, C., Dupont, P., Chipperfield, J., Åkesson, M., Brøseth, H., and Kindberg, J. (2019a). Estimating the size of the scandinavian wolf population with spatial capture recapture and conversion factors. *MINAfagrapport57*, 80pp.

Bischof, R., Milleret, C., Dupont, P., Chipperfield, J., Brøseth, H., and Kindberg, J. (2019b). Estimating density, abundance and population dynamics of bears, wolverines, and wolvesin scandinavia. *MINAfagrapport63*, 79pp.

Bischof, R., Milleret, C., Dupont, P., Chipperfield, J., Tourani, M., Ordiz, A., de Valpine, P., Turek, D., Royle, J. A., Gimenez, O., Flagstad, Ø., Åkesson, M., Svensson, L., Brøseth, H., and Kindberg, J. (2020b). Estimating and forecasting spatial population dynamics of apex predators using transnational genetic monitoring. *Proceedings of the National Academy of Sciences*.

Bischof, R., Turek, D., Milleret, C., Ergon, T., Dupont, P., Dey, S., and de Valpine, P. (2021). *nimbleSCR: Spatial Capture-Recapture (SCR) Methods Using 'nimble'*. R package version 0.1.2.

Chandler, R. B., Hepinstall-Cymerman, J., Merker, S., Abernathy-Conners, H., and Cooper, R. J. (2018). Characterizing spatio-temporal variation in survival and recruitment with integrated population models. *The Auk*, 135(3):409–426.

de Valpine, P., Turek, D., Paciorek, C. J., Anderson-Bergman, C., Lang, D. T., and Bodik, R. (2017). Programming with models: writing statistical algorithms for general model structures with nimble. *Journal of Computational and Graphical Statistics*, 26(2):403–413.

Dey, S., Bischof, R., Dupont, P. P. A., and Milleret, C. (2022). Does the punishment fit the crime? consequences and diagnosis of misspecified detection functions in bayesian spatial capture–recapture modeling. *Ecology and Evolution*, 12(2):e8600.

Dupont, P., Milleret, C., Gimenez, O., and Bischof, R. (2019). Population closure and the bias-precision trade-off in spatial capture–recapture. *Methods in Ecology and Evolution*, 10(5):661–672.

Dupont, P., Milleret, C., Tourani, M., Brøseth, H., and Bischof, R. (2021). Integrating dead recoveries in open-population spatial capture–recapture models. *Ecosphere*, 12(7):e03571.

Ergon, T. and Gardner, B. (2014). Separating mortality and emigration: modelling space use, dispersal and survival with robust-design spatial capture–recapture data. *Methods in Ecology and Evolution*, 5(12):1327–1336.

Flagstad, Ø., Hedmark, E., Landa, A., Brøseth, H., Persson, J., Andersen, R., Segerstrøm, P., and Ellegren, H. (2004). Colonization history and noninvasive monitoring of a reestablished wolverine population. *Conservation Biology*, 18(3):676–688.

Flagstad, , Kleven, O., Brandsegg, H., Spets, M., Eriksen, L., Andersskog, I., Johansson, M., Ekblom, R., Ellegren, H., and Brøseth, H. (2021). Dna-basert overvåking av den skandinaviske jervebestanden 2020. *Norsk institutt for naturforskning(NINA), Trondheim*, NINA Rapport nr 1956.

Gardner, B., Sollmann, R., Kumar, N. S., Jathanna, D., and Karanth, K. U. (2018). State space and movement specification in open population spatial capture-recapture models. *Ecology and Evolution*, 8(20).

Gelman, A. and Rubin, D. (1992). Inference from iterative simulation using multiple sequences. *Statistical Science*, 7:457–511. `http://www.stat.columbia.edu/~gelman/research/published/itsim.pdf`.

Kleven, O., Andersskog, I., Brandsegg, H., Eriksen, L., Spets, M., Königsson, H., Spong, G., Milleret, C., Dupont, P., Bischof, R., Flagstad, , and Brøseth, H. (2022). Dna-basert overvåking av den skandinaviske jervebestanden 2021. *Norsk institutt for naturforskning(NINA),Trondheim*, NINA Rapport nr 2111.

Milleret, C., Bischof, R., Dupont, P., Brøseth, H., Odden, J., and Mattisson, J. (2021a). Gps collars have an apparent positive effect on the survival of a large carnivore. *Biology Letters*, 17(6):20210128.

Milleret, C., Dey, S., Dupont, P., Turek, D., de Valpine, P., and Bischof, R. (2022). Estimating spatially variable and density-dependent survival using open-population spatial capture-recapture models. *bioRxiv*.

Milleret, C., Dupont, P., Chipperfield, J., Turek, D., Brøseth, H., Gimenez, O., de Valpine, P., and Bischof, R. (2020). Estimating abundance with interruptions in data collection using open population spatial capture–recapture models. *Ecosphere*, 11(7):e03172.

Milleret, C., Dupont, P., Åkesson, M., Brøseth, H., Kindberg, J., and Bischof, R. (2021b). Estimates of wolf density, abundance, and population dynamics in scandinavia, 2012 - 2021. *MINAfagrapport72*, 30pp.

Moqanaki, E. M., Milleret, C., Tourani, M., Dupont, P., and Bischof, R. (2021). Consequences of ignoring variable and spatially autocorrelated detection probability in spatial capture-recapture. *Landscape Ecology*, 36(10):2879–2895.

NIMBLE Development Team (2019). *NIMBLE: MCMC, Particle Filtering, and Programmable Hierarchical Modeling*. https://cran.r-project.org/package=nimble.

R Core Team (2018). R: A language and environment for statistical computing. vienna, . *Austria: R Foundation for Statistical Computing.*

Theng, M., Milleret, C., Bracis, C., Cassey, P., and Delean, S. (2022). Confronting spatial capture–recapture models with realistic animal movement simulations. *Ecology*, n/a(n/a):e3676.

Turek, D., Milleret, C., Ergon, T., Brøseth, H., Dupont, P., Bischof, R., and de Valpine, P. (2021). Efficient estimation of large-scale spatial capture–recapture models. *Ecosphere*, 12(2):e03385.

Appendices

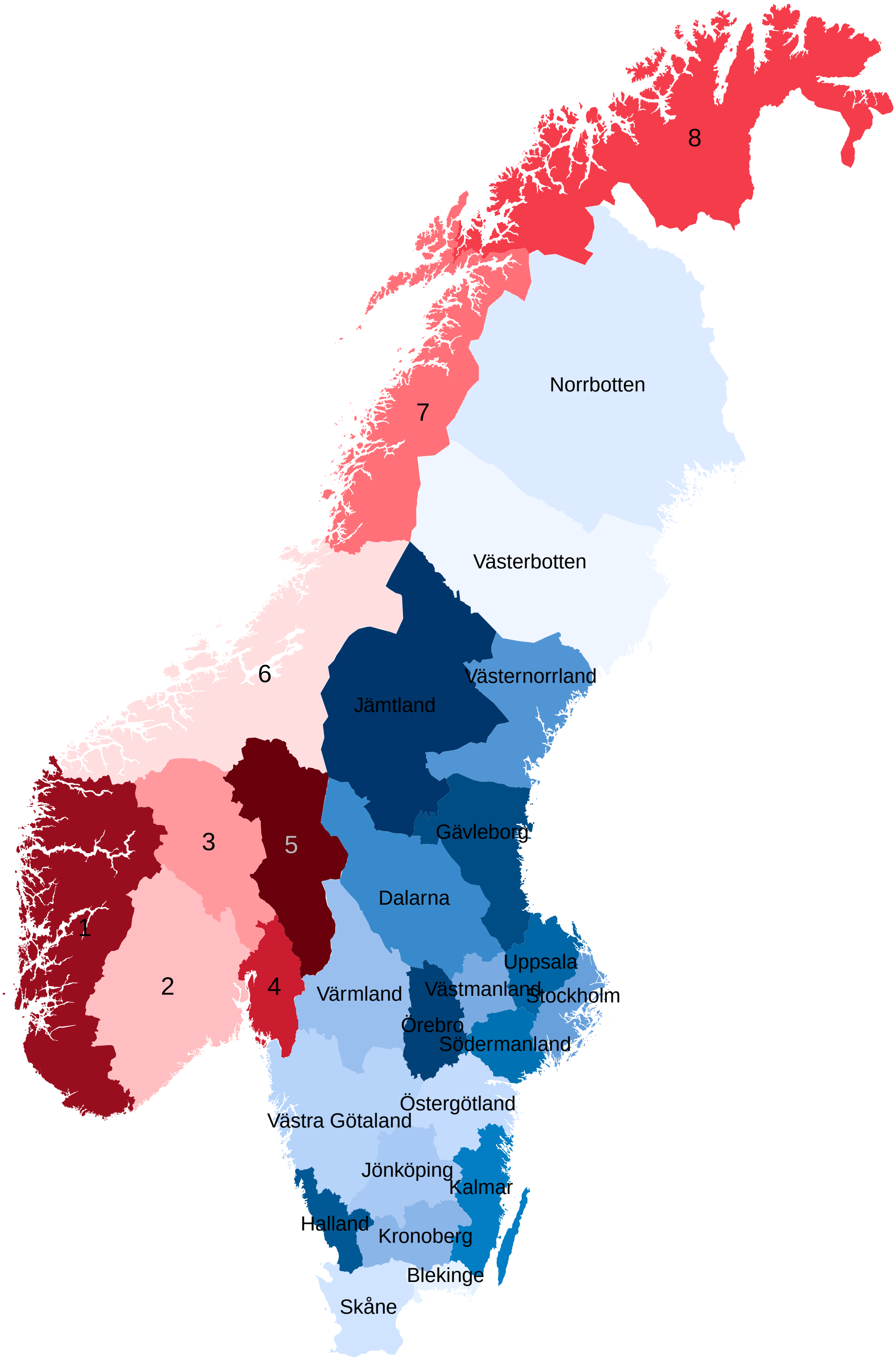

Figure A.1: Management units in Norway (carnivore management regions) and Sweden (counties).

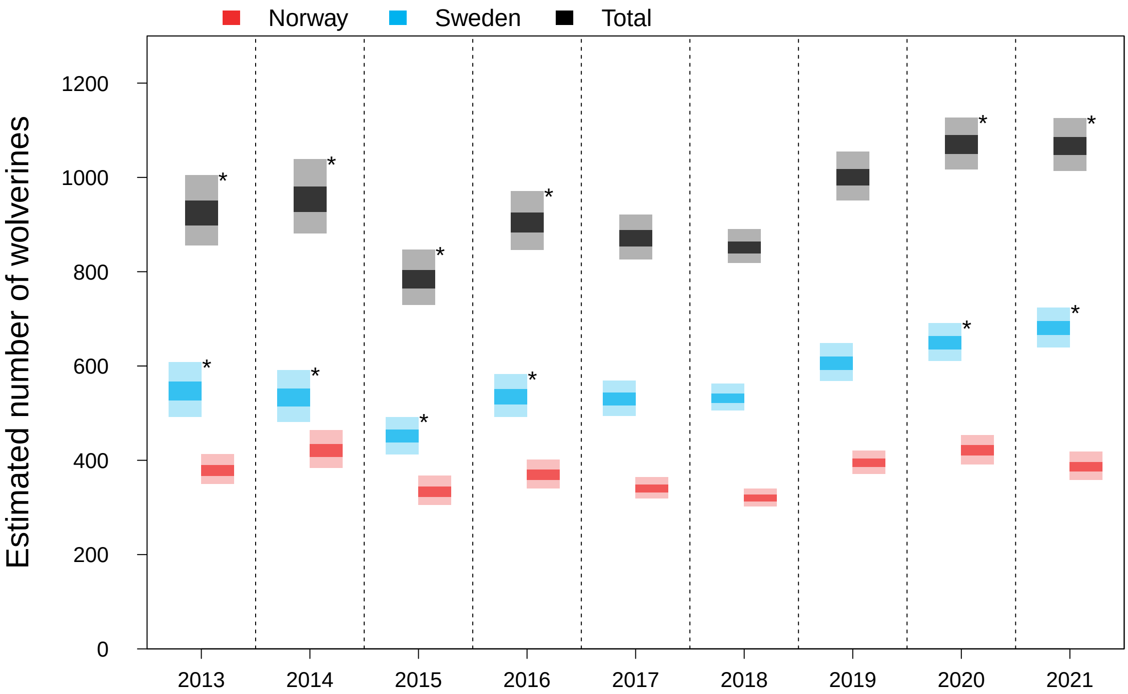

Figure A.2: Total (black) and country-specific (blue: Sweden, red: Norway) annual wolverine population size estimates in Scandinavia between 2013 and 2021. Darker and lighter bars show the 50% and 95% credible intervals, respectively. Bars without a star are based on single-season spatial-capture recapture (SCR) models using wolverine DNA samples. Bars with a star ($*$) are based on a combination of open-population spatial capture-recapture (OPSCR) for Norrbotten county (which was only comprehensively sampled in 2017, 2018, and 2019) and SCR for all other regions.

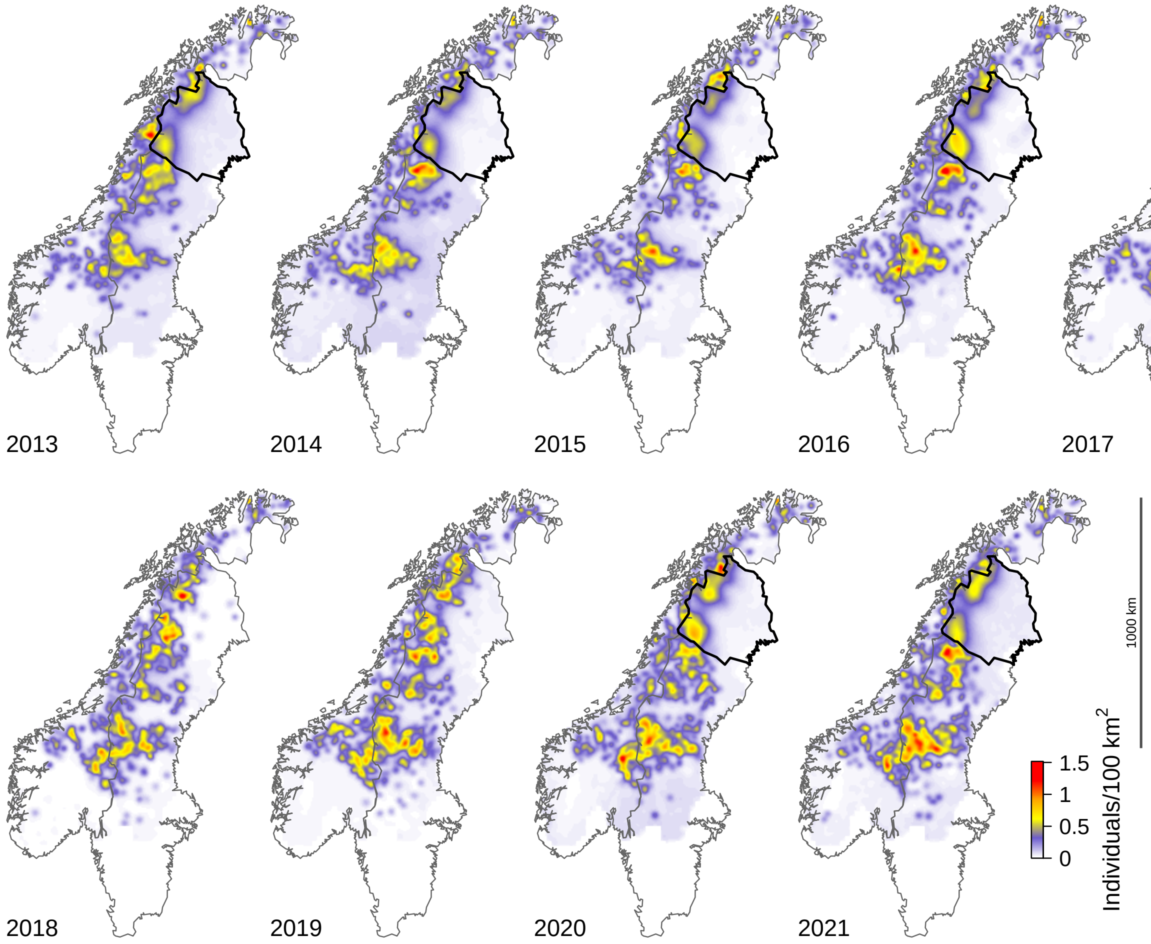

Figure A.3: Wolverine density based on individual utilization distributions throughout the study area in Scandinavia between 2013 and 2021. Density was estimated with single-season spatial-capture recapture models in 2017–2019. Because Norrbotten county was not sampled comprehensively in 2013–2016 and 2020–2021, density in this county were estimated using the open-population spatial capture-recapture (OPSCR) model. Density maps in 2013–2016 and 2020–2021 are therefore a combination of open population spatial-capture recapture models in Norrbotten county (outlined in black) and single-season spatial-capture recapture everywhere else.

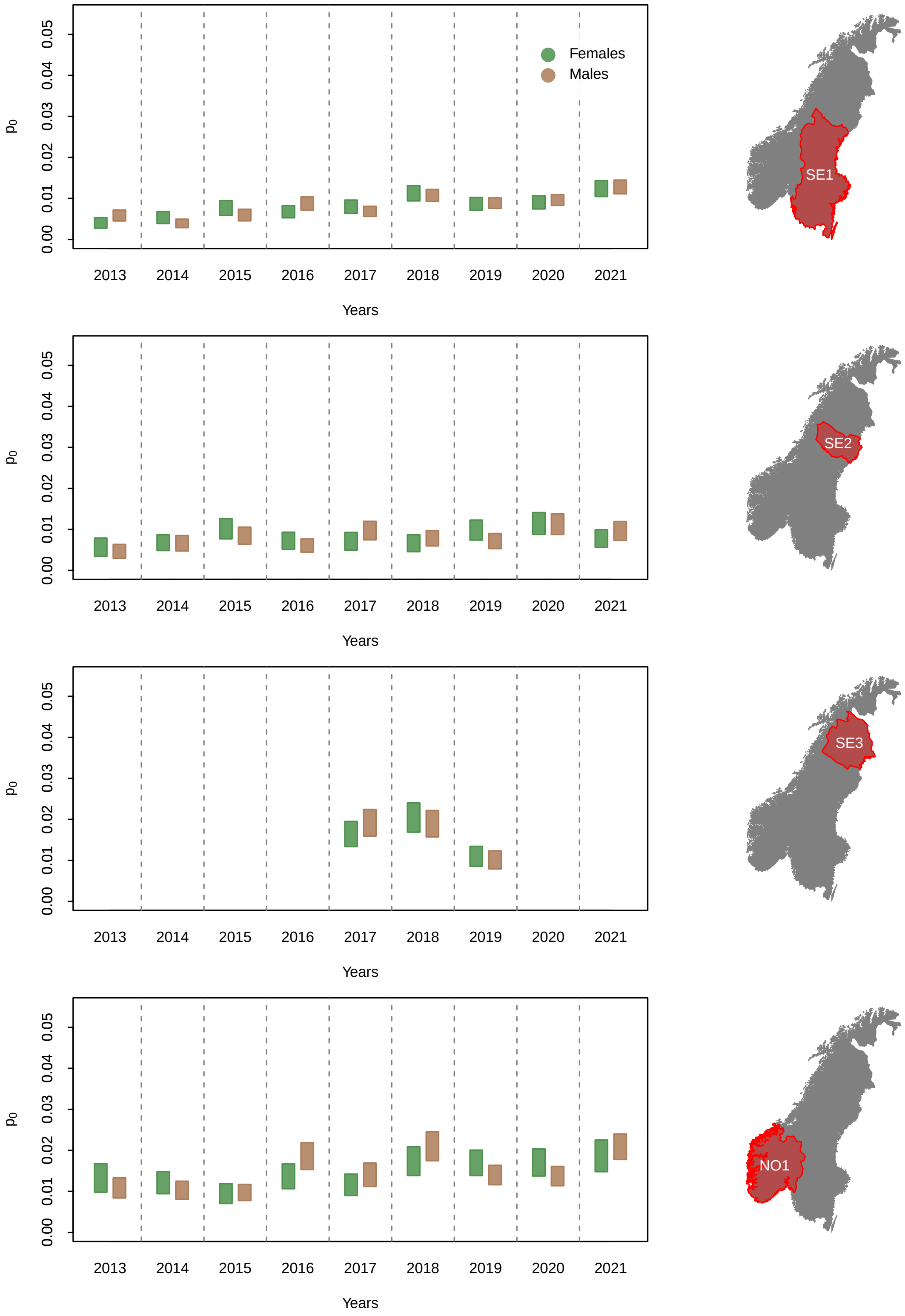

Figure A.4: Baseline detection probability (p_0) estimated by the single-season spatial capture-recapture model. Bars represent 95% credible intervals for males and females. Results are separated into panels based on regions. Estimates are shown for the mean values of the detection covariates. Note that baseline detection probability (p_0) is a theoretical value of detection probability when a detector coincides with the location of an individual's activity center. It is not to be confused with detectability, i.e, the overall probability of detecting an individual.

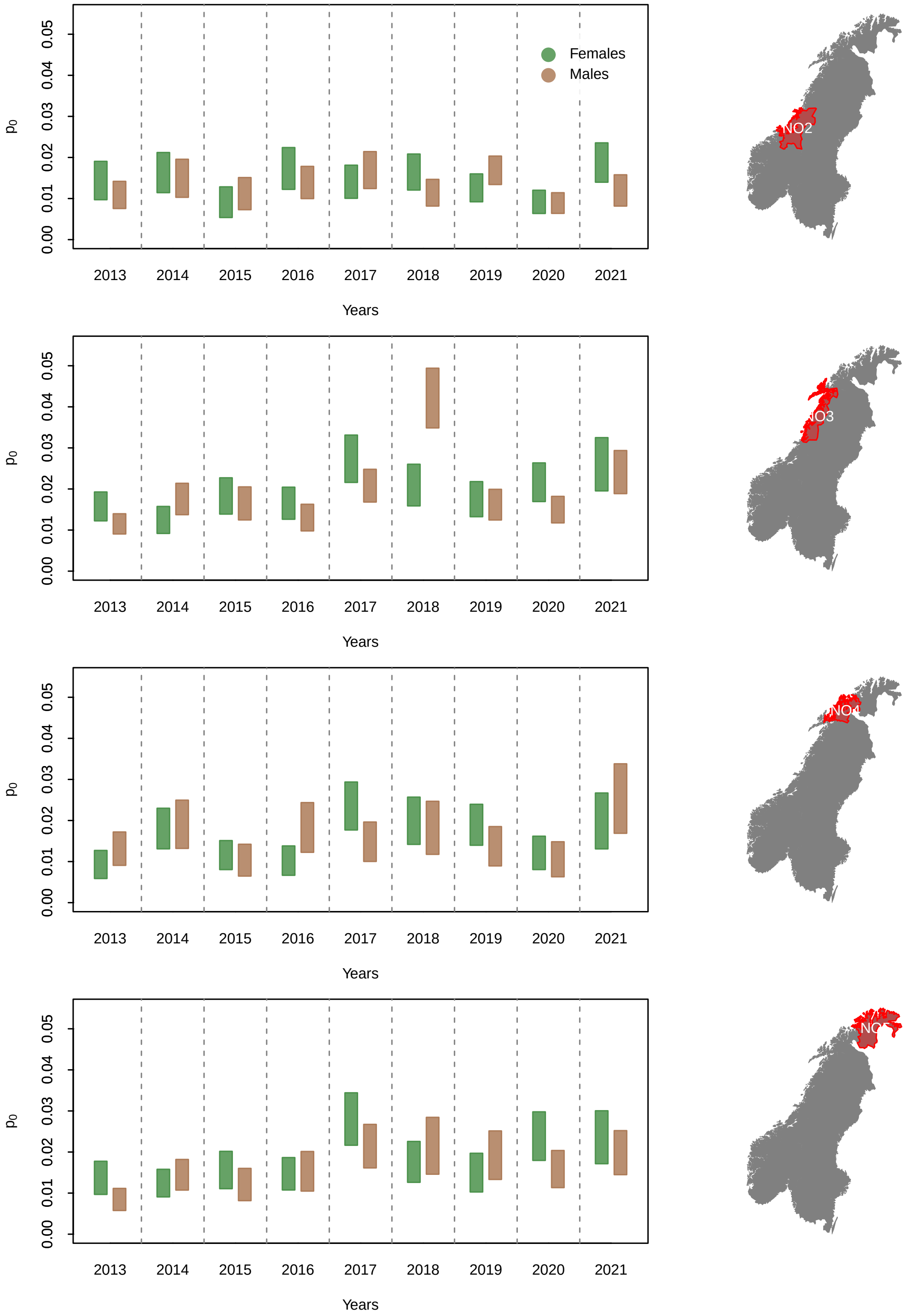

Figure A.4: (continued) Baseline detection probability (p_0) estimated by single-season spatial capture-recapture models. Bars represent 95% credible intervals for males and females. Results are separated into panels based on regions. Estimates are shown for the mean values of the detection covariates. The region "SE3" corresponds to Norrbotten for which p_0 was only estimated in years with comprehensive sampling (2017, 2018 and 2019). For the rest of the years, p_0 in Norrbotten was set to 0. Note that baseline detection probability (p_0) is a theoretical value of detection probability when a detector coincides with the location of an individual's activity center. It is not to be confused with detectability, i.e, the overall probability of detecting an individual.

Table A.1: Annual number of wolverine non-invasive genetic samples included in analysis. Numbers are reported by country, for females (F) and males (M). We included only samples collected within the study area during the primary monitoring period (Dec 1 - Jun 31) between 2013 (2012/13) and 2021 (2020/21).

	2013		2014		2015		2016		2017		2018		2019		2020		2021	
	F	M	F	M	F	M	F	M	F	M	F	M	F	M	F	M	F	M
Norway	458	544	521	578	412	445	468	579	606	670	462	747	592	732	574	684	582	734
Sweden	111	173	186	154	228	221	236	275	487	552	636	839	502	618	351	538	459	558
Total	569	717	707	732	640	666	704	854	1093	1222	1098	1586	1094	1350	925	1222	1041	1292

Table A.2: Annual number of individual wolverines detected via non-invasive genetic sampling and included in analysis. Numbers are reported by country, for females (F) and males (M). We included only individuals associated with samples collected within the study area during the primary monitoring period (Dec 1 - Jun 31) between 2013 (2012/13) and 2021 (2020/21). Some individuals were detected in both countries during the same year, hence the sum of the national counts can exceed the total number of unique individuals detected in Scandinavia.

	2013		2014		2015		2016		2017		2018		2019		2020		2021	
	F	M	F	M	F	M	F	M	F	M	F	M	F	M	F	M	F	M
Norway	174	145	189	135	155	115	180	125	182	132	171	124	192	151	193	152	187	134
Sweden	70	84	85	70	106	86	107	105	211	177	231	211	224	197	170	156	206	165
Total	243	224	271	203	256	194	284	226	377	288	391	317	407	335	358	302	387	293

Table A.3: Number of cause-specific dead recoveries of wolverines in Scandinavia between 2013 and 2021 that were included in the OPSCR analysis. Numbers are reported by country, for females (F) and males (M). Note that dead recovery data from the final season (2021) were not used in this analysis because survival is modeled as part of the transition from one season to the next.

	Country	2013		2014		2015		2016		2017		2018		2019		2020		2021	
		F	M	F	M	F	M	F	M	F	M	F	M	F	M	F	M	F	M
Other	Norway	0	2	1	5	0	2	3	1	3	2	7	1	1	2	2	3	4	3
	Sweden	2	3	1	3	1	2	0	2	0	1	0	1	1	1	0	1	1	1
Legal culling	Norway	45	54	42	34	69	52	42	43	47	61	27	31	57	37	49	63	26	30
	Sweden	9	16	13	8	22	18	6	9	5	2	2	5	6	3	7	19	3	10
Total	Total	56	75	57	50	92	74	51	55	55	66	36	38	65	43	58	86	34	44

Table A.4: Annual abundance estimates for wolverine at three spatial scales: the entire study area, by country, and by management unit. The latter refers to counties ("Län") in Sweden and large carnivore management regions in Norway (Figure A.1). Estimates are based on model-estimated activity center locations. Credible intervals (95%) are shown in parentheses. Small deviations between the total estimate and the sum of abundance estimates from the constituent subregions may arise due to rounding. Values without a star are based on single-season spatial-capture recapture (SCR) models. Estimates for Norrbotten county in years without comprehensive non-invasive genetic sampling were derived using an open-population spatial capture-recapture (OPSCR) model (shown in grey and marked with ∗). Estimates marked with ∗∗ are based on a combination of OPSCR estimates for Norrbotten county and SCR estimates for all other jurisdictions. See Methods section for further detail.

	2013	2014	2015	2016	2017	2018	2019	2020	2021
TOTAL**	925.9 (854-1005)	954.7 (879-1039)	785 (729-847)	904.9 (845-971)	871.1 (826-921)	852.4 (819-891)	1001 (952-1055)	1070.5 (1016-1127)	1067.4 (1013-1126)
NORWAY	378.7 (349-414)	421.2 (384-464)	333.5 (304-367)	369.5 (340-401)	340.2 (318-364)	319.8 (301-340)	394.5 (371-421)	421.2 (392-454)	386.4 (358-418)
Region 1	16.6 (10-25)	27.3 (17-39)	16.4 (10-25)	14 (7-22)	12.9 (7-20)	8.5 (4-14)	10.7 (5-18)	15.2 (7-24)	14.7 (7-23)
Region 2	8.5 (3-16)	16.5 (8-26)	8.3 (3-15)	8.6 (3-15)	8 (3-14)	4.9 (1-10)	6.6 (2-12)	9.7 (4-17)	11.2 (5-18)
Region 3	26.5 (21-33)	37.2 (30-46)	26.3 (20-34)	27.8 (22-35)	25.7 (20-32)	20.9 (17-26)	27.8 (22-34)	31.6 (26-38)	33.5 (28-40)
Region 4	3.9 (1-8)	6.7 (2-12)	3.3 (0-7)	2.8 (0-7)	3.1 (0-7)	1.5 (0-4)	2 (0-5)	6 (2-11)	4 (1-9)
Region 5	58.3 (50-68)	66.3 (56-78)	48.9 (41-58)	59.9 (52-69)	57 (50-66)	66.4 (60-74)	85.5 (78-94)	83.6 (76-92)	81.2 (73-91)
Region 6	72.3 (62-85)	78.6 (66-93)	61.3 (50-74)	75.1 (65-87)	73.7 (64-84)	82.9 (74-93)	98.1 (89-109)	90.7 (78-104)	83.9 (73-96)
Region 7	93.9 (86-103)	70.3 (62-80)	61.8 (55-69)	77 (69-86)	57.8 (52-64)	54.9 (49-61)	68.5 (61-77)	80.5 (72-90)	63.5 (56-72)
Region 8	98.8 (86-113)	118.2 (107-132)	107.1 (95-120)	104.4 (92-119)	101.9 (94-110)	79.8 (70-90)	95.4 (84-108)	103.9 (91-118)	94.4 (82-109)
SWEDEN**	547.2 (491-608)	533.5 (481-591)	451.5 (412-492)	535.4 (491-583)	531 (494-569)	532.6 (505-563)	606.4 (567-648)	649.3 (610-691)	681 (639-724)
Örebro	4.6 (1-9)	7.1 (2-13)	3.7 (0-8)	3.5 (0-8)	3.5 (0-8)	2.9 (1-6)	1.9 (0-5)	6.3 (2-12)	5 (1-10)
Östergötland	0 (0-0)	0 (0-0)	0 (0-0)	0 (0-0)	0 (0-0)	0 (0-0)	0 (0-0)	0 (0-0)	0 (0-0)
Dalarna	31.1 (22-42)	35.7 (25-48)	25 (18-34)	29.6 (22-38)	32.5 (25-41)	41.6 (36-48)	38.5 (32-46)	45.9 (36-56)	51.9 (44-61)
Gävleborg	13.6 (7-21)	17.4 (9-27)	12.7 (7-20)	15.6 (9-23)	14.9 (9-22)	14.9 (11-20)	32.1 (26-38)	31.4 (25-39)	25.3 (20-31)
Jämtland	154.9 (131-183)	157.6 (133-184)	131.6 (113-153)	172.5 (151-196)	157 (140-175)	171.8 (158-187)	190.6 (174-209)	187.3 (171-205)	216.7 (200-234)
Norrbotten*	177.6 (150-208)*	141.2 (119-164)*	139.8 (120-161)*	160.4 (141-181)*	172.9 (158-190)*	158.8 (148-172)*	184.6 (162-209)*	187.9 (165-212)*	183.6 (157-212)*
Södermanland	0.1 (0-1)	0.1 (0-1)	0.1 (0-1)	0.1 (0-1)	0 (0-1)	0 (0-1)	0 (0-1)	0.1 (0-1)	0.1 (0-1)
Värmland	12.8 (7-20)	17 (9-26)	9.2 (4-15)	11 (6-17)	12.8 (8-19)	9.7 (6-14)	7.3 (4-11)	19.6 (13-27)	13.4 (8-20)
Västerbotten	125.2 (101-153)	130.6 (112-151)	108.1 (96-123)	122.6 (104-145)	112.3 (97-129)	100.8 (85-117)	116.7 (102-134)	129.3 (115-145)	140.9 (123-161)
Västernorrland	24.4 (17-33)	22.2 (13-32)	18.7 (12-26)	17.6 (11-25)	22.4 (16-30)	30.7 (25-37)	32.9 (26-40)	37.6 (30-46)	41.1 (34-49)
Västmanland	1.6 (0-4)	2.4 (0-6)	1.3 (0-4)	1.4 (0-4)	1.3 (0-4)	0.8 (0-3)	0.9 (0-3)	2.2 (0-5)	1.6 (0-5)
VästraGötaland	1.4 (0-4)	2.1 (0-6)	1.2 (0-4)	1.2 (0-4)	1.2 (0-4)	0.8 (0-3)	0.9 (0-3)	1.9 (0-5)	1.5 (0-4)

Table A.5: Annual population growth rate estimates for the wolverine population in Scandinavia ("Total") and separately for Norway and Sweden. Estimates were derived using the posterior distribution of annual abundance estimates (Table 1). Credible intervals (95%) are shown in parentheses. Estimates marked with ∗ are based on a combination of OPSCR estimates for Norrbotten county and SCR estimates for all other jurisdictions. See Methods section for further detail.

	2013-2014	2014-2015	2015-2016	2016-2017	2017-2018	2018-2019	2019-2020	2020-2021
Norway	1.11 (0.98-1.26)	0.79 (0.69-0.90)	1.11 (0.97-1.25)	0.92 (0.83-1.02)	0.94 (0.86-1.03)	1.23 (1.13-1.35)	1.07 (0.97-1.18)	0.92 (0.83-1.02)
Sweden	0.98 (0.85-1.12)*	0.85 (0.74-0.97)*	1.19 (1.05-1.34)*	0.99 (0.89-1.11)*	1.00 (0.92-1.09)	1.14 (1.04-1.24)	1.07 (0.97-1.18)*	1.05 (0.97-1.14)*
Total	1.03 (0.92-1.15)*	0.82 (0.74-0.92)*	1.15 (1.04-1.27)*	0.96 (0.88-1.05)*	0.98 (0.91-1.05)	1.17 (1.10-1.26)	1.07 (0.99-1.15)*	1.00 (0.93-1.08)*

Table A.6: Estimates of the demographic parameters obtained from the wolverine OPSCR model. Parameters represent transition rates from Oct 1 to Sep 30 in the following year. Median estimates and 95% credible intervals (in parentheses) for per capita recruitment rate (ρ), survival (ϕ), mortality due to legal culling (h) and mortality due to other causes (w) are presented for males (M) and females (F). Not shown is the scale parameter τ of the function representing inter-annual movement of individuals; Males: τ=32.20km (31.15km-33.22km) and Females: τ =17.68km (17.20km-18.17km).

	2013-2014		2014-2015		2015-2016		2016-2017	
	M	F	M	F	M	F	M	F
ρ	0.27 (0.18-0.36)	0.30 (0.18-0.43)	0.35 (0.26-0.45)	0.19 (0.11-0.28)	0.36 (0.28-0.46)	0.31 (0.22-0.41)	0.39 (0.32-0.47)	0.23 (0.16-0.30)
ϕ	0.50 (0.43-0.56)	0.64 (0.58-0.71)	0.63 (0.57-0.70)	0.75 (0.69-0.80)	0.64 (0.58-0.70)	0.82 (0.76-0.87)	0.66 (0.60-0.71)	0.78 (0.73-0.83)
h	0.15 (0.11-0.18)	0.08 (0.06-0.11)	0.08 (0.05-0.11)	0.08 (0.05-0.10)	0.15 (0.12-0.19)	0.10 (0.08-0.13)	0.11 (0.08-0.15)	0.06 (0.05-0.09)
w	0.35 (0.29-0.42)	0.27 (0.20-0.34)	0.29 (0.22-0.35)	0.18 (0.12-0.23)	0.21 (0.15-0.27)	0.08 (0.04-0.13)	0.23 (0.17-0.28)	0.15 (0.11-0.20)

	2017-2018		2018-2019		2019-2020		2020-2021	
	M	F	M	F	M	F	M	F
ρ	0.37 (0.32-0.43)	0.24 (0.18-0.29)	0.43 (0.37-0.49)	0.28 (0.22-0.33)	0.41 (0.35-0.47)	0.24 (0.18-0.29)	0.28 (0.23-0.33)	0.24 (0.18-0.30)
ϕ	0.63 (0.57-0.68)	0.76 (0.71-0.80)	0.69 (0.63-0.74)	0.83 (0.78-0.88)	0.64 (0.58-0.69)	0.76 (0.70-0.81)	0.52 (0.46-0.58)	0.71 (0.64-0.78)
h	0.12 (0.09-0.16)	0.06 (0.05-0.09)	0.08 (0.06-0.11)	0.04 (0.03-0.06)	0.08 (0.06-0.11)	0.07 (0.05-0.09)	0.14 (0.11-0.18)	0.06 (0.05-0.08)
w	0.25 (0.21-0.30)	0.18 (0.13-0.22)	0.23 (0.18-0.28)	0.13 (0.08-0.18)	0.28 (0.23-0.34)	0.18 (0.12-0.23)	0.33 (0.28-0.39)	0.23 (0.16-0.30)

Table A.7: Estimates of the spatial and detection process parameters obtained from the nine single-season SCR models (one per year) for male (M) and female (F) wolverines in Scandinavia. β represents the effect of the number of known wolverine dens on AC locations (Bischof et al., 2020b). The scale parameter σ of the detection function is expressed in kilometers. β_1 corresponds to the effect of previous detection of an individual on detection probability (p_0), β_2 to the effect of search-effort (track length) on detection probability (p_0), β_3 to the effect of distance to the nearest roads on detection probability (p_0), and β_4 to the effect of average snow cover during the monitoring period on detection probability (p_0). Coefficients are associated with scaled covariates. Credible intervals (95%) are shown in parentheses.

	2013		2014		2015		2016		2017	
	M	F	M	F	M	F	M	F	M	F
β	0.59 (0.49-0.69)	0.64 (0.52-0.75)	0.55 (0.44-0.66)	0.56 (0.45-0.65)	0.63 (0.52-0.74)	0.66 (0.55-0.76)	0.68 (0.59-0.78)	0.66 (0.56-0.77)	0.60 (0.51-0.68)	0.67 (0.59-0.75)
σ	8.80 (8.33-9.32)	6.27 (5.83-6.74)	8.41 (7.97-8.88)	6.09 (5.73-6.50)	8.77 (8.31-9.26)	5.97 (5.60-6.36)	8.42 (8.03-8.86)	6.35 (5.96-6.77)	8.52 (8.20-8.88)	6.79 (6.49-7.12)
β_1	0.37 (0.16-0.59)	0.13 (-0.16-0.42)	0.60 (0.38-0.82)	0.00 (-0.27-0.26)	0.31 (0.09-0.54)	0.17 (-0.09-0.44)	0.63 (0.43-0.82)	0.16 (-0.11-0.43)	0.51 (0.35-0.68)	0.05 (-0.14-0.22)
β_2	0.33 (0.26-0.40)	0.41 (0.32-0.52)	0.44 (0.37-0.53)	0.51 (0.42-0.60)	0.42 (0.33-0.52)	0.37 (0.28-0.47)	0.39 (0.32-0.46)	0.49 (0.39-0.61)	0.36 (0.30-0.42)	0.33 (0.27-0.39)
β_3	-0.11 (-0.26-0.04)	-0.06 (-0.24-0.11)	0.15 (0.02-0.29)	-0.06 (-0.20-0.10)	0.07 (-0.11-0.24)	-0.14 (-0.31-0.03)	0.01 (-0.13-0.14)	-0.09 (-0.25-0.06)	-0.05 (-0.13-0.03)	0.02 (-0.06-0.10)
β_4	-0.05 (-0.21-0.12)	0.19 (0.01-0.37)	0.55 (0.23-0.85)	0.64 (0.35-0.96)	0.09 (-0.12-0.29)	0.44 (0.23-0.65)	0.03 (-0.18-0.23)	0.14 (-0.07-0.35)	0.30 (0.13-0.46)	0.22 (0.05-0.38)

	2018		2019		2020		2021	
	M	F	M	F	M	F	M	F
β	0.62 (0.54-0.70)	0.65 (0.58-0.73)	0.60 (0.53-0.68)	0.67 (0.59-0.74)	0.61 (0.51-0.70)	0.56 (0.47-0.65)	0.58 (0.49-0.67)	0.63 (0.54-0.71)
σ	8.29 (8.02-8.58)	6.52 (6.23-6.82)	7.85 (7.55-8.16)	5.99 (5.71-6.29)	8.19 (7.86-8.54)	6.60 (6.29-6.96)	8.17 (7.86-8.49)	6.66 (6.34-7.01)
β_1	0.76 (0.61-0.91)	0.18 (0.00-0.37)	0.64 (0.47-0.81)	0.17 (-0.02-0.35)	0.31 (0.14-0.47)	0.07 (-0.13-0.28)	0.47 (0.30-0.64)	0.01 (-0.20-0.22)
β_2	0.32 (0.27-0.38)	0.34 (0.27-0.41)	0.42 (0.35-0.49)	0.51 (0.43-0.60)	0.34 (0.29-0.40)	0.48 (0.40-0.56)	0.50 (0.43-0.58)	0.54 (0.45-0.62)
β_3	-0.17 (-0.25-(-)0.09)	-0.10 (-0.19-(-)0.01)	-0.09 (-0.19-0.01)	-0.01 (-0.10-0.09)	-0.17 (-0.31-(-)0.03)	-0.23 (-0.38-(-)0.08)	0.04 (-0.09-0.18)	0.02 (-0.11-0.15)
β_4	0.11 (0.00-0.22)	0.14 (0.01-0.28)	-0.13 (-0.28-0.03)	-0.03 (-0.22-0.15)	0.40 (0.23-0.57)	0.66 (0.44-0.89)	0.15 (0.02-0.28)	0.26 (0.11-0.42)

Table A.8: Average proportion of individuals detected via non-invasive genetic sampling (NGS) in Scandinavia. Values were calculated as the number of individuals detected with NGS (Table A.2) divided by the total and sex-specific abundance estimates obtained from combining SCR and OPSCR models (Table A.4). Credible intervals (95%) are shown in parentheses.

	2013	2014	2015	2016	2017	2018	2019	2020	2021
M	0.62 (0.56-0.68)	0.56 (0.49-0.63)	0.65 (0.58-0.71)	0.66 (0.60-0.72)	0.87 (0.83-0.92)	0.91 (0.86-0.95)	0.84 (0.79-0.89)	0.68 (0.63-0.73)	0.71 (0.66-0.77)
F	0.40 (0.34-0.46)	0.40 (0.35-0.46)	0.47 (0.42-0.54)	0.45 (0.40-0.51)	0.70 (0.64-0.76)	0.78 (0.73-0.83)	0.68 (0.63-0.73)	0.51 (0.47-0.56)	0.53 (0.48-0.58)
Total	0.48 (0.43-0.53)	0.46 (0.41-0.50)	0.53 (0.49-0.58)	0.52 (0.48-0.57)	0.76 (0.72-0.81)	0.83 (0.79-0.86)	0.74 (0.70-0.78)	0.58 (0.54-0.62)	0.60 (0.56-0.63)